

A multi-grain model for migration recrystallization in polar ice

R. STAROSZCZYK

*Institute of Hydro-Engineering, Polish Academy of Sciences
Kościerska 7, 80-328 Gdańsk, Poland
e-mail: rstar@ibwpan.gda.pl*

IN THE PAPER A MULTI-GRAIN MODEL for a migration recrystallization phenomenon in polar ice is presented. A single crystal of ice is treated as a transversely isotropic and incompressible medium which deforms by viscous creep. The anisotropic viscous behaviour of the ice crystal is described by a constitutive law that includes three microscopic viscosity parameters, and the macroscopic behaviour of the polycrystal is derived by adopting the Taylor–Voigt approximation of the velocity gradient homogeneity in the material. It is assumed that recrystallize, that is gradually disappear, these crystals which are most stressed, and at their expense new crystals are nucleated with the orientations that enhance the deformation of the polycrystal. The model predictions are illustrated by results of numerical simulations of simple flows, showing the evolution of the oriented structure of ice and the variation of macroscopic viscosities with increasing strains.

Key words: polar ice, evolving anisotropy, micro-structure, migration recrystallization, recrystallization wave.

Copyright © 2009 by IPPT PAN

Notations

A, B	ice crystal dimensionless rheological parameters,
\mathbf{c}	crystal c -axis unit vector,
\mathbf{D}	strain-rate tensor,
E_a, E_s	enhancement factors for compression and shear,
\mathbf{I}	unit tensor,
\mathbf{L}	velocity gradient tensor,
\mathbf{M}	structural tensor,
\mathbf{R}	rotation matrix,
S_{eq}	equivalent deviatoric stress,
\mathbf{S}	deviatoric Cauchy stress tensor,
\mathbf{v}	velocity vector,
\mathbf{W}	spin tensor,
x_i ($i = 1, 2, 3$)	global spatial Cartesian co-ordinates,
x_i^c ($i = 1, 2, 3$)	local spatial Cartesian co-ordinates,
ζ	normalized equivalent deviatoric stress,
θ	angle defining the crystal c -axis orientation,
κ	shear strain,

λ_i ($i = 1, 2, 3$)	principal stretches,
μ	viscosity for shear on a crystal basal plane,
μ_0	isotropic polycrystalline ice viscosity,
μ_{ij} ($i, j = 1, 2, 3$)	anisotropic ice crystal viscosities,
φ	angle defining the crystal c -axis orientation.

1. Introduction

Ice core samples drilled from polar ice sheets in Antarctica and Greenland reveal strong anisotropic fabrics, shown by a significant re-alignment of initially randomly oriented individual ice crystals (GOW *et al.* [14], THORSTEINSSON *et al.* [21]). Progressive re-orientation of crystal c -axes (the axes of ice crystal hexagonal symmetry), taking place in the polycrystalline material in its response to changing deformation and stress conditions as ice particles descend from the free surface to depth, leads to considerable changes in ice macroscopic viscosities on different shear planes. The main micro-process that induces the development of the oriented structure in the polar ice is the crystal lattice rotation by intracrystalline slip (AZUMA and HIGASHI [2], ALLEY [1]). This process operates throughout the entire path of the ice descent from the free surface to depth, and gives rise, in the absence of other micro-mechanisms, to very strong single-maximum fabrics, with the majority of the crystal c -axes clustered along the vertical (ALLEY [1]).

However, besides the above lattice rotation mechanism, the polar ice is also subject to several recrystallization processes which affect its micro-structure. One such a mechanism, the so-called normal crystal growth process, due to its isotropic character, has no influence on the macroscopic anisotropy of ice. Another mechanism, known as the rotation recrystallization (or polygonization), is most active in the middle part of an ice sheet, and results in bending and subsequent splitting of the ice grains into new ones, with their orientations being very close to those of existing grains (the latter do not disappear). Therefore, the macroscopic effect of this mechanism is only a slight modification of the anisotropic properties of ice. As ice particles, during their further downward motion, enter the bottom part of a glacier and approach its base, in certain conditions yet another recrystallization process may activate, due to which the structure of ice changes dramatically, as evidenced by multi-maxima fabrics, with very coarse and interlocking grains, found near the glacier base (DUVAL [6], DUVAL and CASTELNAU [8], DE LA CHAPELLE *et al.* [5], DUVAL *et al.* [7]). Such a process, known in glaciology as the migration (or dynamic) recrystallization, is caused by rapid migration of grain boundaries between highly deformed and dislocation-free crystals, and leads to the nucleation of new grains at the expense of old ones (which eventually disappear). Not all the factors which initiate and subsequently control the migration recrystallization mechanism have

been identified yet, but it seems that the most important among them are: high, that is near-melting temperature (above -10°C), high deviatoric stress, strain, and strain-rate magnitudes, with some role also played by the bed topography (DE LA CHAPELLE *et al.* [5], DUVAL *et al.* [7]). The macroscopic result of the migration recrystallization, due to the changes induced in the ice microstructure, is a significant modification of ice viscosities compared to those of the non-recrystallized ice. Therefore, this process has a crucial effect on the overall flow of polar ice sheets, since the latter deform mainly by shearing in near-base regions, that is, in the regions in which the recrystallized ice fabrics are observed.

To date only few theoretical attempts have been made to describe the process of migration recrystallization. VAN DER VEEN and WHILLANS [22] have developed a multi-grain, uniform-stress model in which the onset of the process is described by two alternative criteria, both based on macroscopic strains in the polycrystalline aggregate (by construction, in this formulation the stress dependence of the recrystallization process cannot be captured, since all crystals in the aggregate are assumed to be equally stressed). STAROSZCZYK and MORLAND [20] have proposed a phenomenological constitutive model, in which, ignoring most of the micro-processes underlying the fabric evolution in ice, the onset of the migration recrystallization is described in terms of a temperature-dependent critical macroscopic strain-rate invariant. Subsequently, MORLAND [17] has formulated a model in which the onset of recrystallization is related to a temperature-dependent critical lattice distortion parameter, equivalent to a condition on a stored mechanical energy of dislocations. An approach, based on the cellular automata method, which incorporates several types of recrystallization, including the migration one, has been developed by KTITAREV *et al.* [15] and FARIA *et al.* [11]. The model, however, is restricted to one-dimensional deformations, therefore it cannot be used in realistic ice sheet flow simulations. Quite a distinct approach has been pursued by FARIA *et al.* [10] to construct a general theory of recrystallization processes in a polycrystalline material by treating it as a mixture of continuous diversity and making use of the general principles of thermodynamics. This theory, applied to polycrystalline ice, has been substantially extended by FARIA [9]. However, this general model, due to a multitude of material parameters entering the constitutive laws and difficulties associated with their quantitative determination, will hardly find implementation in ice sheet flow modelling in a foreseeable future.

In the present paper the migration recrystallization phenomenon is described by extending a multi-grain formulation by STAROSZCZYK [18, 19], in its earlier version accounting only for the lattice rotation mechanism. In that constitutive model, based on the Taylor–Voigt approximation of a uniform velocity gradient

within a polycrystalline aggregate, the macroscopic behaviour of ice is derived by a simple homogenization method, by which the macroscopic response is a mean average of microscopic responses of a finite number of discrete grains (assumed to have equal volumes) representing the aggregate. The behaviour of each crystal in the aggregate is followed separately by one another; that is, no crystal interactions are accounted for. In the model, a single crystal of ice is treated as a transversely isotropic and incompressible body which deforms by viscous creep. The viscous response of the crystal is described by a constitutive law that involves three viscosity parameters which define different shear resistances of the crystal in different glide directions.

Now the previous formulation is extended to include the recrystallization as well. For this purpose, it is assumed that recrystallize these crystals in an aggregate which are most stressed, as postulated by DE LA CHAPELLE *et al.* [5]. Hence, a parameter is introduced that defines a critical level of the deviatoric stress invariant, and it is supposed that a given crystal starts to recrystallize as soon as the microscopic stress invariant for that crystal reaches the above critical value. A new crystal is nucleated from that undergoing recrystallization in a smooth, continuous manner – in other models based on the multi-grain approach (VAN DER VEEN [22], KTITAREV *et al.* [15]) it has been assumed that the process occurs abruptly, that is, within one discrete time step. The orientations of new grains (their c -axes) are chosen in a way that is most favourable for their microscopic deformations. Hence, three different hypotheses are adopted, and then discussed in Sec. 3, concerning the initial spatial orientation of the c -axes of newly developing grains.

The model predictions are illustrated by results of numerical simulations carried out for sustained uni-axial compression and simple shear flows, demonstrating the evolution of the oriented structure (c -axes distribution) in recrystallizing polycrystalline ice, and comparing these predictions with the corresponding results when no recrystallization takes place. Further, the variations of instantaneous macroscopic viscosities with increasing deformations, for the above three hypotheses and different critical deviatoric stress-invariant levels, are shown to display some characteristic features of the macroscopic anisotropy evolution in a polycrystalline ice aggregate.

2. Governing equations

This section summarizes some theoretical results concerning the ice crystal lattice rotation model, which are relevant in the context of the migration recrystallization formulation proposed further in this work. For detailed derivation of these results, and their discussion, the Reader is referred to earlier works of the author [18, 19].

2.1. Single crystal kinematics

Due to the transverse isotropy of the elementary hexagonal crystal of ice, with the axis of rotational symmetry coinciding with the crystal c -axis, the changing position of the crystal in space can be uniquely defined by the orientation of a unit vector aligned along the c -axis. Hence, we introduce a unit vector \mathbf{c} along the crystal c -axis, and two angles: the zenith angle θ ($0 \leq \theta \leq \pi/2$) and the longitude (azimuth) angle φ ($0 \leq \varphi \leq 2\pi$), which define the orientation of the crystal in a fixed rectangular Cartesian reference frame Ox_i ($i = 1, 2, 3$), see Fig. 1. Since in some instances it is more convenient to describe macroscopic properties of a single crystal in a reference frame associated with that crystal, rather than in the global co-ordinates Ox_i , we also adopt a local rectangular frame Ox_i^c ($i = 1, 2, 3$), moving together with the crystal. The axes of the local frame are chosen in such a way that x_3^c coincides with the direction of the c -axis (vector \mathbf{c}), x_1^c lies in the plane $Ox_3x_3^c$, and x_2^c has the direction that preserves the right-handedness of the local co-ordinate system. All tensor quantities whose components are expressed in the local frame will be indicated by the superscript ‘c’, and those expressed in the global frame will be left without any suffix.

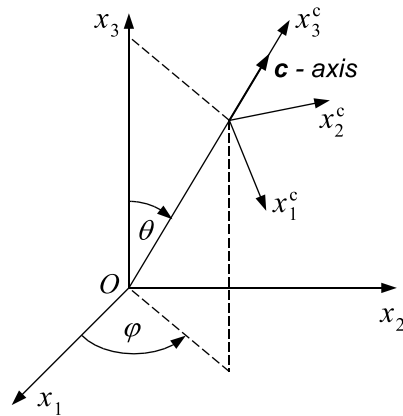


FIG. 1. Global and local co-ordinate systems, with the zenith angle θ and the longitude angle φ defining the changing crystal c -axis orientation in space.

Transformation of components of non-scalar quantities from the local to the global reference frame is described by means of the rotation matrix \mathbf{R} , the components of which are defined by

$$(2.1) \quad \mathbf{R} = \begin{pmatrix} \cos \theta \cos \varphi & -\sin \varphi & \sin \theta \cos \varphi \\ \cos \theta \sin \varphi & \cos \varphi & \sin \theta \sin \varphi \\ -\sin \theta & 0 & \cos \theta \end{pmatrix}.$$

Since the local frame Ox_i^c moves relative to the fixed global frame Ox_i , the above rotation matrix is time-dependent. Hence, the position vectors in both co-ordinate systems, \mathbf{x} and \mathbf{x}^c , are related by

$$(2.2) \quad \mathbf{x} = \mathbf{R}(t) \mathbf{x}^c, \quad \mathbf{x}^c = \mathbf{R}^T(t) \mathbf{x},$$

where \mathbf{R}^T is the transpose of \mathbf{R} , and t denotes time. Further, by (2.2)₁, the components of the velocity vectors, \mathbf{v} and \mathbf{v}^c , transform by

$$(2.3) \quad \mathbf{v} = \dot{\mathbf{x}} = \dot{\mathbf{R}}\mathbf{x}^c + \mathbf{R}\mathbf{v}^c,$$

where the superposed dots denote time derivatives. Differentiation of the latter equation with respect to the co-ordinates x_i ($i = 1, 2, 3$) yields the expression which connects the spatial velocity gradients \mathbf{L} and \mathbf{L}^c (with components $L_{ij} = \partial v_i / \partial x_j$ and $L_{ij}^c = \partial v_i^c / \partial x_j^c$, respectively), measured in both reference frames, in the form:

$$(2.4) \quad \mathbf{L} = \dot{\mathbf{R}}\mathbf{R}^T + \mathbf{R}\mathbf{L}^c\mathbf{R}^T.$$

By taking the symmetric and anti-symmetric parts of \mathbf{L} and \mathbf{L}^c , relation (2.4) furnishes the transformation rules for the strain-rate tensors, \mathbf{D} and \mathbf{D}^c , and the spin tensors, \mathbf{W} and \mathbf{W}^c , expressed by

$$(2.5) \quad \mathbf{D} = \mathbf{R}\mathbf{D}^c\mathbf{R}^T, \quad \mathbf{W} = \dot{\mathbf{R}}\mathbf{R}^T + \mathbf{R}\mathbf{W}^c\mathbf{R}^T.$$

The tensor relation (2.5)₂ is equivalent to three equations for non-trivial components of \mathbf{W} in terms of three non-zero components of \mathbf{W}^c : W_{12}^c , W_{13}^c and W_{23}^c . The first component, W_{12}^c , is irrelevant to this analysis, as it describes the rotation of the crystal about its axis of symmetry (which does not affect the viscous behaviour of the crystal); hence, the respective equation for the $(\)_{12}$ components can be ignored here. The other two spin tensor components, W_{13}^c and W_{23}^c , can be expressed in terms of the strain-rate tensor components by assuming that the grain basal planes remain parallel to each other during the viscous deformation of the crystal. This provides two kinematic relations (MEYSSONNIER and PHILIP [16]):

$$(2.6) \quad W_{13}^c = D_{13}^c, \quad W_{23}^c = D_{23}^c.$$

Accordingly, on account of (2.6), the tensor expression (2.5)₂ yields the following two evolution equations:

$$(2.7) \quad \dot{\theta} = -D_{13}^c + W_{13} \cos \varphi + W_{23} \sin \varphi,$$

$$(2.8) \quad \dot{\varphi} \sin \theta = -D_{23}^c - W_{12} \sin \theta - (W_{13} \sin \varphi - W_{23} \cos \varphi) \cos \theta$$

for the rotation-rates of the two angles, θ and φ , defining the current orientation of the crystal c -axis, in terms of two microscopic strain-rates and three microscopic spins. In the Taylor-Voigt approach adopted in this work, all the five latter variables will be expressed in terms of the macroscopic strain-rates and spins.

2.2. Constitutive relation for a crystal

In derivation of the constitutive law for the viscous creep of a single hexagonal crystal of ice it has been assumed that the crystal is transversely isotropic about its c -axis, is incompressible, and can deform by slips on the basal (normal to the c -axis) and prismatic (parallel to the c -axis) planes. The frame-indifferent linearly viscous flow law, formulated in the global co-ordinate system Ox_i , and expressing the microscopic deviatoric stress \mathbf{S} in terms of the microscopic strain-rate \mathbf{D} , is then given by the equation (STAROSZCZYK [18]):

$$(2.9) \quad \mathbf{S} = 2\mu \left\{ \frac{1}{2} (3A + B - 4) \operatorname{tr}(\mathbf{MD})(\mathbf{M} - \frac{1}{3} \mathbf{I}) + BD \right. \\ \left. + (1 - B) [\mathbf{MD} + \mathbf{DM} - \frac{2}{3} \operatorname{tr}(\mathbf{MD}) \mathbf{I}] \right\}.$$

In the above equation, \mathbf{M} is a structure tensor that describes the transverse symmetry of the material, and is defined by

$$(2.10) \quad \mathbf{M} = \mathbf{c} \otimes \mathbf{c}, \quad M_{ij} = c_i c_j \quad (i, j = 1, 2, 3),$$

where c_i ($i = 1, 2, 3$) are the components of the c -axis unit vector \mathbf{c} , tr denotes the trace operator, and \mathbf{I} is the unit tensor.

The constitutive law (2.9) includes three microscopic viscosity parameters: μ , A and B . The first one, μ , is the viscosity for the glide on the crystal basal plane, i.e. it is the viscosity μ_{13} for shearing in the plane $Ox_1^c x_3^c$ in the local frame attached to the crystal. The other two rheological parameters, A and B , are dimensionless quantities that define the degree of the single crystal anisotropy. These two parameters relate the axial viscosity μ_{33} (for compression along the axis x_3^c), and the prismatic shear viscosity μ_{12} (for shearing in the plane $Ox_1^c x_2^c$), to the viscosity μ_{13} :

$$(2.11) \quad A = \frac{\mu_{33}}{\mu_{13}}, \quad B = \frac{\mu_{12}}{\mu_{13}}.$$

Since $\mu = \mu_{13}$ is the smallest possible viscosity in the crystal, it follows that $A \geq 1$ and $B \geq 1$. The case of $A = B = 1$ describes an isotropic crystal, with equal viscosities for all deformation modes, while the limit case of $A \rightarrow \infty$ and $B \rightarrow \infty$ describes a crystal which can deform only by basal glide.

2.3. Macroscopic behaviour of a polycrystal

All macroscopic quantities, describing the behaviour of a polycrystalline aggregate as a whole, are distinguished from those referring to an individual crystal by superposing a bar on a respective symbol. Thus, $\bar{\mathbf{D}}$ is the macroscopic strain-rate, as opposed to the microscopic strain-rate \mathbf{D} , etc.

In the adopted multi-grain formulation, the macroscopic response of the polycrystalline aggregate, consisting, at a given material point and at a given time instant, of N_c discrete grains, is defined as the sum of microscopic contributions of all constituent grains. It is assumed that discrete crystals, the number of which varies in time as recrystallizing crystals disappear and new ones nucleate, can have different volumes (which change continuously during the recrystallization process) – this is an extension of the previous theory (STAROSZCZYK [18]) in which the number of grains was fixed and all crystals had the same, constant in time, volumes. Accordingly, the components of any macroscopic tensor entity $\bar{\mathbf{T}}$ are defined as weighted arithmetic averages of respective components of microscopic tensor entities $\mathbf{T}^{(k)}$ ($k = 1, 2, \dots, N_c$). That is,

$$(2.12) \quad \bar{T}_{ij} = \frac{1}{V_0} \sum_{k=1}^{N_c} V_k T_{ij}^{(k)}, \quad V_0 = \sum_{k=1}^{N_c} V_k,$$

where V_k denotes the volume of a k -th discrete grain, and V_0 is the total volume of all grains in the aggregate.

The Taylor–Voigt approximation of the uniformity of the velocity gradient within the polycrystalline aggregate is expressed by

$$(2.13) \quad \mathbf{L} = \bar{\mathbf{L}},$$

which is equivalent to nine kinematic relations connecting microscopic and macroscopic quantities. The condition (2.13) necessarily implies that

$$(2.14) \quad \mathbf{D} = \bar{\mathbf{D}} \quad \text{and} \quad \mathbf{W} = \bar{\mathbf{W}}.$$

The microscopic constitutive law (2.9), with the relation (2.14)₁, expresses the microscopic stresses in terms of the macroscopic strain-rate. Assume that an isotropic polycrystal contains an infinite number of crystals, with their c -axis orientations uniformly distributed in space. Then the averaging relation (2.12), used for the stresses, relates the macroscopic stress to the macroscopic strain-rate, and hence determines the macroscopic viscosity, μ_0 , in terms of the microscopic rheological parameters μ , A and B :

$$(2.15) \quad \mu_0 = \frac{\mu}{5} (A + 2B + 2).$$

The above expression represents the upper bound on the macroscopic viscosity of the polycrystalline ice aggregate. The lower bound can be determined by

applying another classical homogenization method, that is, the Sachs-Reuss approximation of the stress homogeneity within the aggregate, expressed by the condition $\mathbf{S} = \bar{\mathbf{S}}$ (VAN DER VEEN and WHILLANS [22], GÖDERT and HUTTER [13], O. GAGLIARDINI and J. MEYSSONNIER [12], STAROSZCZYK [19]).

As the polycrystal is subject to the deformation under sustained uni-axial compression or simple shear, then all crystal c -axes gradually rotate to eventually align in one direction. In this limit situation, the properties of the polycrystal become the same as those of the single monocrystal, the viscous behaviour of which is described by the constitutive law (2.9). Accordingly, the latter law gives

$$(2.16) \quad \frac{\mu_{13}}{\mu_0} = \frac{5}{A + 2B + 2} = \frac{1}{E_s}, \quad \frac{\mu_{33}}{\mu_0} = \frac{5A}{A + 2B + 2} = \frac{1}{E_a}.$$

The parameters E_s and E_a introduced in the above viscosity ratios are known in glaciology as the enhancement factors for shear and compression, respectively, and are measured in laboratory tests (BUDD and JACKA [3]). Thus, the above two expressions can be used to correlate the macroscopic quantities, E_s and E_a , with the microscopic quantities, A and B , to yield:

$$(2.17) \quad A = \frac{E_s}{E_a}, \quad B = \frac{5E_s}{2} - \frac{E_s}{2E_a} - 1.$$

For polar ice, the typical values of the enhancement factors are $E_s = 5$ and $E_a = 1/3$. With the latter magnitudes, relations (2.17) determine the values of the microscopic viscosity parameters as $A = 15$ and $B = 4$. It is worth noting here that none of the uniform stress formulations mentioned above enables the correlation of the observed enhancement factors with the microscopic parameters describing the single crystal of ice.

3. Migration recrystallization mechanism description

Two essential ingredients of the recrystallization model are (1) – the criterion which defines the onset of the recrystallization process, and (2) – the determination of the initial orientation of a newly created ice grain. As already mentioned in the Introduction, the major factors which trigger the migration recrystallization are high temperature and high levels of stress, strain or strain-rate. In this study we neglect the effect of temperature, assuming that the process occurs at constant temperature, and also assume that the process is controlled by the stress only, excluding from the analysis other possible factors. Hence, we adopt a microscopic stress measure expressed by the second principal invariant of the deviatoric stress tensor \mathbf{S} , defined by

$$(3.1) \quad S_{\text{eq}}^2 = J_2 = \frac{1}{2} S_{ij} S_{ij} \quad (i, j = 1, 2, 3),$$

where S_{eq} is termed the equivalent micro-stress, and the summation convention for repeated indices applies. Further, we introduce a critical magnitude of the equivalent micro-stress, $S_{\text{eq}}^{\text{cr}}$, and suppose that a given crystal k ($k = 1, 2, \dots, N_c$) undergoes recrystallization as long as the equivalent micro-stress in that crystal is greater than, or equal to, the critical equivalent stress level. That is, when the following condition is satisfied:

$$(3.2) \quad S_{\text{eq}}^{(k)} \geq S_{\text{eq}}^{\text{cr}}.$$

In order to include in future formulations the influence of temperature on the recrystallization mechanism, one could incorporate the dependence of the above critical stress measure on the absolute temperature (by making $S_{\text{eq}}^{\text{cr}}$ to decrease as ice temperature increases above some critical temperature level – below that critical level no recrystallization occurs). An approach similar to the above was applied in the phenomenological recrystallization model by STAROSZCZYK and MORLAND [20].

The other crucial component of the recrystallization model concerns the determination of the spatial orientations of new grains which nucleate from those undergoing the migration recrystallization. It is commonly accepted (BUDD and JACKA [3], ALLEY [1], VAN DER VEEN and WHILLANS [22], DE LA CHAPELLE *et al.* [5]) that new crystals of ice are oriented in a way that is most favourable for their further deformation (which is the easiest by slip on the basal planes). That is, a newly grown grain is least stressed in a current stress configuration – this follows from the fact that the most stressed grains, due to their orientation in the ice polycrystal, are those which deform at the smallest rates (so-called ‘hard’ grains), and vice versa, the least stressed grains are those deforming at largest rates (so-called ‘soft’ grains) (DE LA CHAPELLE *et al.* [5]).

Accordingly, in the earlier discrete-grain models (VAN DER VEEN and WHILLANS [22], D. KTITAREV *et al.* [15]) it has been assumed that the preferred direction of the c -axis of a newly nucleated crystal is such that its crystal basal plane is parallel to the plane of the maximum macroscopic shear stress in a polycrystal. In general (when all three principal macroscopic stresses are different from one another), there are only two such planes, both with the normals being at the angles of 45° to the principal axes of the maximum and minimum compressive stresses in the aggregate, which admit only two possible directions for the c -axes of new crystals. This seems to be a kind of restriction on possible orientations of the new crystal c -axes, since many crystals would then have very similar orientations, aligned along certain directions, whereas the observed recrystallized polar ice fabrics always show some scatter in the c -axes distributions. For this reason, the latter restriction is relaxed here by allowing the new crystal c -axes to align along all directions (not only along the two ones, as above) at the angle of 45° to the maximum compressive stress axis. Another possibility, which will

be investigated here, is to attempt to find, for a given stress configuration, an optimal c -axis direction, that is, to find a spatial orientation at which the crystal microscopic deviatoric stress invariant reaches the minimum value. This can be difficult to perform for a general viscous flow field; therefore it has been done below for two simpler flow regimes: uni-axial compression and simple shear.

First consider the uni-axial compression flow. Assuming that the axial compression is carried out along the co-ordinate axis x_3 , then, due to the axial symmetry of the flow, and the ice incompressibility condition $\text{tr } \bar{\mathbf{D}} = 0$, the macroscopic, equal to the microscopic, strain-rate tensor is defined by

$$(3.3) \quad \bar{\mathbf{D}} = \mathbf{D} = \begin{pmatrix} -\frac{1}{2}D_{33} & 0 & 0 \\ 0 & -\frac{1}{2}D_{33} & 0 \\ 0 & 0 & D_{33} \end{pmatrix}.$$

Consider a crystal of the spatial orientation defined by the angles φ and θ . Then the c -axis unit vector is given by

$$(3.4) \quad \mathbf{c} = (\sin \theta \cos \varphi, \sin \theta \sin \varphi, \cos \theta)^T,$$

which determines, by the definition (2.10), the structure tensor \mathbf{M} in terms of φ and θ . Inserting now the strain-rate \mathbf{D} , defined by (3.3), and the latter structure tensor \mathbf{M} into the constitutive equation (2.9) yields the microscopic stress tensor \mathbf{S} . The components of this stress determine, by (3.1), the equivalent stress S_{eq} as a function of the orientation angles φ and θ , the crystal rheological parameters μ , A and B , and the strain-rate component D_{33} . For convenience, the resulting microscopic stress S_{eq} is normalized by means of the magnitude of the macroscopic equivalent stress, \bar{S}_{eq} , for an isotropic polycrystalline aggregate which deforms at the same strain-rates, given by (3.3). The stress \bar{S}_{eq} is a function of the macroscopic viscosity μ_0 and the strain-rate D_{33} (for the isotropic polycrystal the law $\bar{\mathbf{S}} = 2\mu_0\bar{\mathbf{D}}$ applies); subsequently, μ_0 is eliminated by employing (2.15). The above-described calculations result in the following dimensionless relation:

$$(3.5) \quad \zeta = \frac{S_{\text{eq}}}{\bar{S}_{\text{eq}}} \\ = \frac{5}{2(A + 2B + 2)} [3(A^2 + B^2) \sin^4 \theta + 6A^2 \cos^4 \theta + 3 \sin^2 2\theta - 2A^2]^{1/2},$$

where ζ denotes the normalized equivalent deviatoric stress in a crystal, expressed in terms of the two rheological parameters A and B , defining the strength of anisotropy of the crystal, and the c -axis zenith angle θ (due to the rotational symmetry of the uni-axial flow, the above relation for ζ is independent of the longitude angle φ).

It can be easily seen that for an isotropic crystal, described by $A = B = 1$, relation (3.5) gives $\zeta = S_{\text{eq}}/\bar{S}_{\text{eq}} = 1$, which means that all crystals in the aggregate are equally stressed. In the limit case of crystals deforming only by basal glide, described by $A \rightarrow \infty$ and $B \rightarrow \infty$, relation (3.5) yields

$$(3.6) \quad \frac{S_{\text{eq}}}{\bar{S}_{\text{eq}}} \rightarrow \frac{5}{6} [4 - 3 \sin^2(2\theta)]^{1/2}.$$

The latter gives the maximum normalized equivalent stress equal to $5/3$ for the crystal c -axis oriented at either $\theta = 0$ or $\theta = 90^\circ$ (hard crystals), and the minimum value of this stress equal to $5/6$ for $\theta = 45^\circ$ (soft crystal). These predictions are in very good quantitative agreement with the results presented by DE LA CHAPELLE *et al.* [5], obtained by applying a visco-plastic self-consistent model by CASTELNAU *et al.* [4], in which the resistance of non-basal slip systems was assumed to be 70 times larger than that of basal slip. Also, it follows from (3.5) that for $\theta = 0$, for any combinations of A and B , the equivalent stress $S_{\text{eq}}/\bar{S}_{\text{eq}}$ is equal to $1/E_a$, the reciprocal of the axial enhancement factor.

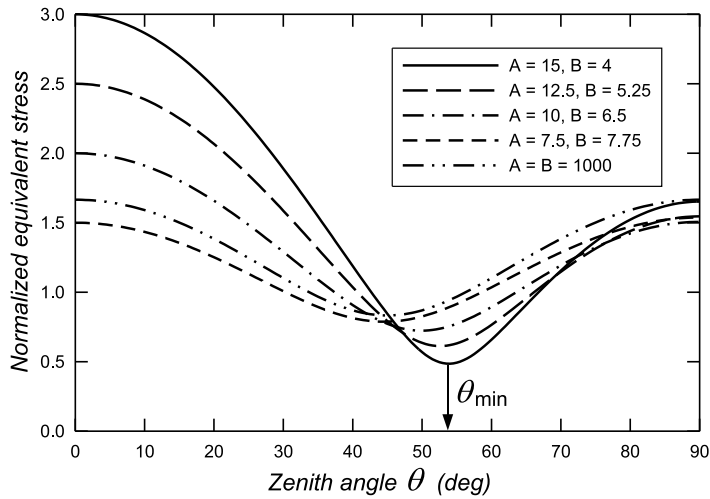


FIG. 2. Normalized equivalent stress ζ in uni-axial compression as a function of the c -axis zenith angle θ and the crystal rheological parameters A and B .

The variation of the equivalent stress $\zeta = S_{\text{eq}}/\bar{S}_{\text{eq}}$ with the crystal c -axis zenith angle θ , for different combinations of the microscopic rheological parameters A and B , is illustrated in Fig. 2. It is seen that, depending on the strength of anisotropy of the crystal (defined by the parameters A and B), the most favourable orientation for the crystal c -axis in a polycrystalline ice aggregate under uni-axial compression is that defined by the zenith angles θ by a few degrees larger than 45° . For the rheological parameters $A = 15$ and $B = 4$, best

correlating with the observed macroscopic properties of polar ice, the optimal inclination of the crystal, denoted by θ_{\min} , is at the angle of 53.86° to the axis of the macroscopic compressive stress.

Next consider the simple shear configuration. Assuming that the deformation takes place in the plane Ox_1x_3 , the macroscopic and microscopic strain-rate tensors are given by

$$(3.7) \quad \bar{\mathbf{D}} = \mathbf{D} = \begin{pmatrix} 0 & 0 & D_{13} \\ 0 & 0 & 0 \\ D_{13} & 0 & 0 \end{pmatrix}.$$

Proceeding in the way analogous to that applied to the uni-axial compression flow and described in the text below equation (3.4), with the strain-rate component D_{33} replaced now by D_{13} , we arrive at the expression

$$(3.8) \quad \zeta = \frac{S_{\text{eq}}}{\bar{S}_{\text{eq}}} = \frac{5}{2(A + 2B + 2)} \\ \times \{(3A^2 + B^2) \sin^2 2\theta \cos^2 \varphi + 4[(B^2 \sin^2 \theta + \cos^2 \theta) \sin^2 \varphi + \cos^2 2\theta \cos^2 \varphi]\}^{1/2},$$

which describes the dependence of the normalized equivalent stress in simple shear on the rheological parameters A and B and the crystal c -axis orientation angles θ and φ .

It follows from (3.8) that for the crystal c -axis aligned along the x_3 -axis, $\theta = 0$, and for $\theta = 90^\circ$ and either $\varphi = 0$ or $\varphi = 180^\circ$, that is for the c -axis along the x_1 -axis, the equivalent stress $S_{\text{eq}}/\bar{S}_{\text{eq}}$ reaches its minimum value equal to $1/E_s$, the reciprocal of the shear enhancement factor. This means that in the simple shear configuration, the most favourably oriented crystals are those with the c -axes lying on the shear plane Ox_1x_3 and inclined at the angle 45° to the principal axis of compression. Figure 3 illustrates the dependence of the normalized equivalent stress on the angles θ and φ , for the rheological parameters $A = 15$ and $B = 4$. Only the range $0 \leq \varphi \leq \pi/2$ is considered, due to the symmetry property $\zeta(\theta, \varphi) = \zeta(\theta, \pi - \varphi)$ (the plot is symmetric about the co-ordinate line $\varphi = \pi/2$). It is seen in the contour plot that the most poorly oriented grains (most stressed) are those aligned along the directions defined by $\theta = 45^\circ$ and either $\varphi = 0$ or $\varphi = 180^\circ$ (for the adopted values of A and B , the normalized equivalent stress reaches then the magnitude of ~ 2.63). The first of the latter two directions is normal, and the other is parallel, to the direction of the principal axis of compression in the simple shear configuration assumed.

In the following section the proposed migration recrystallization model will be used in numerical simulations to investigate the development of anisotropic fabrics in polycrystalline ice. The three above-discussed hypotheses regarding the initial orientations of newly created grains will be investigated. These hypotheses can be summarized as follows:

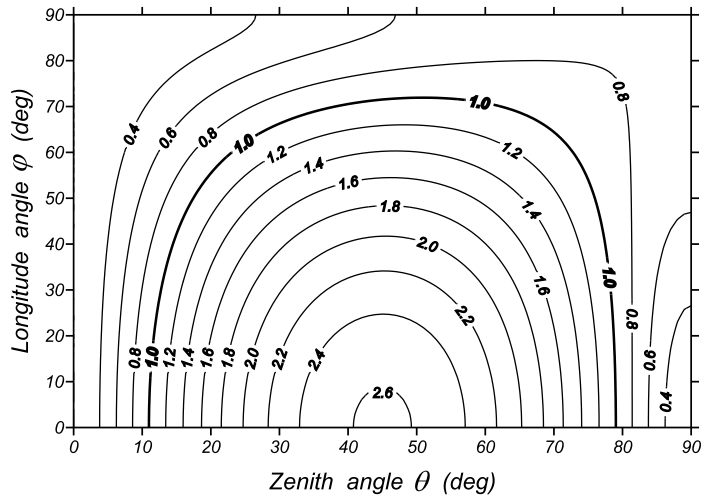


FIG. 3. Normalized equivalent stress ζ in simple shear as a function of the c -axis orientation angles θ and φ , for the crystal rheological parameters $A = 15$ and $B = 4$.

1. The c -axis of a new crystal is normal to the plane of the maximum macroscopic shear stress. In general, there are only two such planes, and this orientation (of the two) is chosen which is closer to that of the old crystal.
2. The c -axis of a new crystal lies on a conical surface at the angle 45° to the principal axis of the maximum macroscopic compressive stress, and an orientation is chosen which is the closest to that of the old grain.
3. The c -axis of a new crystal is on a conical surface at the angle θ_{\min} to the principal axis of the maximum macroscopic compressive stress, and an orientation is chosen which is the closest to that of the old grain.

Hence, three cases, corresponding to the above three hypotheses, have been implemented in the multi-grain model constructed to simulate the recrystallization process.

4. Flow simulations

The proposed migration recrystallization formulation has been used to simulate numerically the viscous behaviour of polycrystalline ice in two simple regimes: uni-axial compression and simple shear. The simulations have been performed for the rheological parameters pertaining to polar ice, and for the strain-rate magnitudes typically occurring in flows of large polar ice sheets. Hence, the macroscopic viscosity of the isotropic ice has been adopted as $\mu_0 = 25 \text{ MPa} \cdot \text{yr}$, where the unit ‘yr’ denotes the year, and the enhancement factors have been assumed as $E_a = 1/3$ and $E_s = 5$, yielding the microscopic parameter values $A = 15$ and $B = 4$. The axial strain-rate in the direction of compression

has been $\overline{D}_{33} = 10^{-4} \text{ yr}^{-1}$, and the shear strain-rate in the plane of shearing has been $\overline{D}_{13} = 10^{-4} \text{ yr}^{-1}$, both assumed constant throughout the simulations. The calculations have been conducted by adopting in the initial configuration $N_c = 1000$ discrete grains of equal volumes, with a random distribution of the grain c -axes, to represent a macroscopically isotropic polycrystalline aggregate.

There is some difficulty associated with the proper estimation of the recrystallization time for a crystal, due to the lack of relevant data in the literature. DE LA CHAPELLE [5] give the value of 2400 years needed for a crystal to subdivide due to the process of rotation recrystallization (polygonization). However, the latter process takes place in middle regions of ice sheets, with typical temperatures (around -30° C) much lower than those (above -10° C) in the near-bottom regions in which migration recrystallization occurs. Thus, due to this temperature difference, it has been supposed that the latter process requires less time to recrystallize a grain than the polygonization mechanism. Hence, a value of 1000 years has been adopted in calculations, though the arbitrariness of this choice is realized.

First consider unconfined uni-axial compression flow. Assuming that the compression is carried out along the co-ordinate axis x_3 , then, due to the axial symmetry of the flow, the strains along the lateral directions x_1 and x_2 are equal. Assuming the material co-ordinate axes X_i ($i = 1, 2, 3$) to be parallel to the respective spatial co-ordinates x_i , the deformation field is defined by

$$(4.1) \quad x_1 = \lambda_1 X_1, \quad x_2 = \lambda_2 X_2, \quad x_3 = \lambda_3 X_3, \quad \lambda_1 = \lambda_2 = \lambda_3^{-1/2},$$

where λ_i ($i = 1, 2, 3$) are the principal stretches along the x_i axes, all equal to unity at the start of deformation from the isotropic state, and $\lambda_3 < 1$ subsequently. The last relation in (4.1) is due to the incompressibility condition $\lambda_1 \lambda_2 \lambda_3 = 1$. Differentiation with respect to time and then to the spatial co-ordinates x_i , of the above expressions, yields the macroscopic velocity gradient $\overline{\mathbf{L}}$, strain-rate $\overline{\mathbf{D}}$, and spin $\overline{\mathbf{W}}$ tensors given by

$$(4.2) \quad \overline{\mathbf{L}} = \overline{\mathbf{D}} = \begin{pmatrix} -\frac{1}{2}\dot{\lambda}_3/\lambda_3 & 0 & 0 \\ 0 & -\frac{1}{2}\dot{\lambda}_3/\lambda_3 & 0 \\ 0 & 0 & \dot{\lambda}_3/\lambda_3 \end{pmatrix}, \quad \overline{\mathbf{W}} = \mathbf{O}.$$

The evolution of the anisotropic ice fabric under uni-axial compression is illustrated in Fig. 4, showing the distributions of the crystal c -axes by means of the Schmidt diagrams (equal area pole diagrams). Each dot in the diagrams represents the position at which an individual crystal c -axis intersects the surface of a unit hemisphere (when each c -axis passes through the centre of the sphere), projected onto the plane Ox_1x_2 . The diagrams demonstrate how the ice fabric

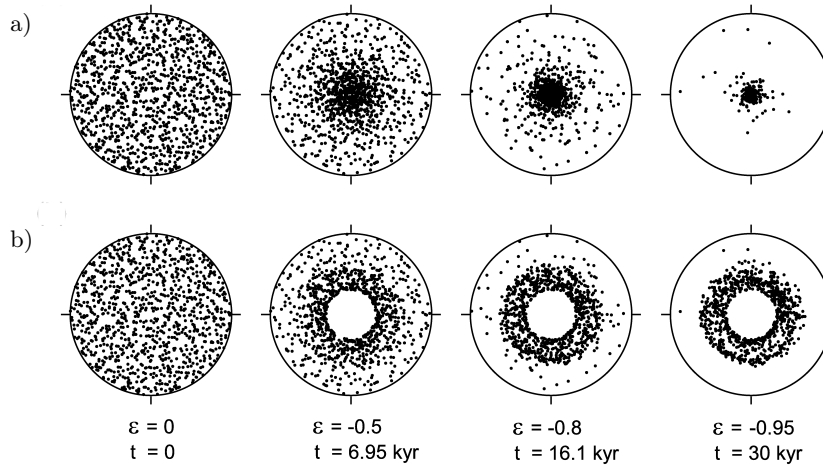


FIG. 4. Evolution of fabric in uni-axial compression along the x_3 -axis as a function of the macroscopic axial strain $\varepsilon = \lambda_3 - 1$ and time t (in thousands of years) for:
a) non-recrystallizing and b) recrystallizing ice.

changes with an increasing axial strain $\varepsilon = 1 - \lambda_3$, given in the figure, together with the times t (given in thousands of years) at which that axial strain has been reached.

The upper row of diagrams, (a), shows the evolution of the c -axis distribution when no recrystallization occurs; thus, only the crystal lattice rotation mechanism operates. It is seen how, due to the latter mechanism, individual crystals rotate and gradually cluster around the axis of compression (which is normal to the plane of plots), giving rise to a strong single-maximum fabric at large axial deformations. For comparison, the lower row of diagrams, (b), shows the evolution of fabric when the migration recrystallization process takes place, acting alongside the crystal lattice rotation process. The presented plots have been obtained by applying the hypothesis (3) for the new crystal orientation, by which new crystals are initially (before they start to rotate) aligned at the optimal angle $\theta_{\min} = 53.86^\circ$ to the compression axis. It has been assumed that the crystal recrystallization starts when the equivalent stress ratio $\zeta^{\text{cr}} = S_{\text{eq}}^{\text{cr}} / \bar{S}_{\text{eq}}$ is equal to 2.2. This particular threshold stress level has been chosen on the basis of experimental observations by BUDD and JACKA [3], indicating that typical fabrics formed in recrystallizing ice under uni-axial compression have girdles at the angle of about 25° to the compression axis. This means that all grains with the orientation angles $\theta \lesssim 25^\circ$ recrystallize. Fig. 2 shows (see the curve for $A = 15$ and $B = 4$) that the equivalent stress level which corresponds to that limit angle $\theta = 25^\circ$ is equal to about 2.2, hence the choice of the above value of $\zeta^{\text{cr}} = 2.2$. The diagrams in Fig. 4b for the ice undergoing recrystallization show that characteristic features of a girdle fabric start to appear at the axial

strain as small as $\varepsilon = -0.5$ (two-fold axial compression of ice), and subsequently fully develop with increasing deformation, which is illustrated by the strong girdle fabric corresponding to the strain $\varepsilon = -0.95$ (twenty-fold compression of ice, which is a typical magnitude for bottom layers in polar ice masses). The c -axes distributions resulting from applying the other two hypotheses for the new grain orientations, (1) and (2), are qualitatively very similar, differing only in the size of the girdles around the axis of compression: the girdle diameters become smaller due to the smaller initial inclination of the new grains to that axis (45° instead of $\theta_{\min} \sim 54^\circ$).

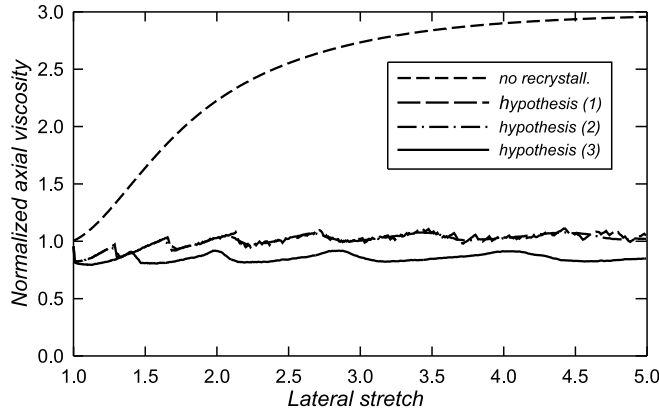


FIG. 5. Variation of the normalized axial viscosity μ_{33}/μ_0 with the lateral stretch λ_1 in uni-axial compression for non-recrystallizing ice, and for recrystallizing ice with three different hypotheses on new crystal orientations.

In the context of the polar ice sheet flow modelling, more important than the differences in qualitative properties of recrystallizing and non-recrystallizing ice fabrics are the respective differences between the macroscopic viscosities of ice. Figure 5 illustrates the evolution of the normalized axial viscosities μ_{33}/μ_0 as a function of the lateral stretch λ_1 , obtained by applying the three hypotheses for the new grain initial orientation. These viscosities are compared with the viscosity of non-recrystallizing ice. We note that the viscosities of ice undergoing recrystallization vary with its deformation in a non-monotonic manner, displaying a kind of a wave-like pattern. This is because at the beginning of deformation, performed at a constant rate, there is a certain number of grains (around 10% of the total number) which immediately start to recrystallize. These recrystallizing grains give rise to a group of newly nucleated grains at very similar orientations with respect to the axis of compression. As the polycrystal continues to deform, these newly formed grains, due to the crystal lattice rotation process, gradually approach unfavourable orientations at which the microscopic critical stress level is reached, resulting in the whole group of crystals starting to recrystallize again

at about the same time, etc. Such ‘recrystallization waves’ have been mentioned by DUVAL and CASTELNAU [8] as a possible mechanism occurring in ice, producing a sequence of softening/hardening phases experienced by ice during its creep.

It follows from Fig. 5 that the hypothesis (3), with the optimal orientation of the newly formed crystals defined by the angle θ_{\min} , predicts the macroscopic axial viscosity which is smaller than that of the isotropic ice, with the average value $\mu_{33}/\mu_0 \sim 0.85$. Compared to (3), the hypotheses (1) and (2) lead to the ice fabrics which are only slightly harder, with the average macroscopic viscosities $\mu_{33}/\mu_0 \sim 1.02$, that is, practically those of the isotropic ice. STAROSZCZYK and MORLAND [20] have assumed in their phenomenological theory that the normalized macroscopic axial viscosity of recrystallizing ice becomes unity – on the basis of the above results this seems to be a very good approximation. There are some small differences, seen in Fig. 5, between the viscosities yielded by the hypotheses (1) and (2), both requiring new crystals to align at 45° to the compression axis. The simulations have revealed that the hypothesis (1), apparently due to its restrictiveness as to the spatial orientation of a new crystal, has a tendency of increasing any small material asymmetry that initially exists in a polycrystalline aggregate. As a consequence, the predicted fabrics show, at large strains, some forms of a more general anisotropy than the form which could be expected to develop in a given stress/deformation configuration.

Figure 6 shows how the macroscopic axial viscosities are affected by the magnitude of the critical equivalent stress. Hence, the dimensionless viscosities μ_{33}/μ_0 , plotted against the lateral stretch λ_1 , and obtained by adopting the hypothesis (3), are displayed for different values of the stress ratio $\zeta^{\text{cr}} = S_{\text{eq}}^{\text{cr}}/\bar{S}_{\text{eq}}$.

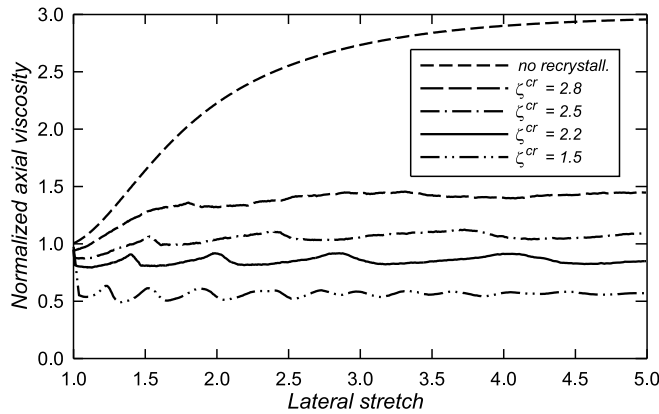


FIG. 6. Variation of the normalized axial viscosity μ_{33}/μ_0 with the lateral stretch λ_1 in uni-axial compression for non-recrystallizing ice, and for recrystallizing ice with the hypothesis (3) on new crystal orientations, for different critical equivalent stresses ζ^{cr} .

We note that the wave-like character of the viscosity plots becomes more pronounced with a decreasing level of the critical recrystallization stress, with more dramatic, and frequent, changes in the viscosities occurring at smaller strains. For the particular values of ζ^{cr} illustrated in the figure, the average macroscopic viscosities (for the stretches $\lambda_1 \geq 2$) vary from $\mu_{33}/\mu_0 \sim 1.36$ for $\zeta^{\text{cr}} = 2.8$, to the value ~ 0.57 for $\zeta^{\text{cr}} = 1.5$. For comparison, the minimum possible macroscopic axial viscosity μ_{33}/μ_0 is equal to about 0.49, which follows from Fig. 2, or Eq. (3.5), and would be attained if all crystals in the aggregate were inclined at the optimal angle θ_{min} to the axis of macroscopic compression.

Next consider a simple shear in the plane Ox_1x_3 , starting from an initially isotropic state. The deformation field is then described by

$$(4.3) \quad x_1 = X_1 + \kappa X_3, \quad x_2 = X_2, \quad x_3 = X_3,$$

where κ is a shear strain, increasing monotonically from zero. Time and space differentiation of the above expressions results in the macroscopic velocity gradient, strain-rate and spin tensors given by

$$(4.4) \quad \bar{\mathbf{L}} = \begin{pmatrix} 0 & 0 & \dot{\kappa} \\ 0 & 0 & 0 \\ 0 & 0 & 0 \end{pmatrix}, \quad \bar{\mathbf{D}} = \begin{pmatrix} 0 & 0 & \frac{1}{2}\dot{\kappa} \\ 0 & 0 & 0 \\ \frac{1}{2}\dot{\kappa} & 0 & 0 \end{pmatrix}, \quad \bar{\mathbf{W}} = \begin{pmatrix} 0 & 0 & \frac{1}{2}\dot{\kappa} \\ 0 & 0 & 0 \\ -\frac{1}{2}\dot{\kappa} & 0 & 0 \end{pmatrix}.$$

The development of fabric with increasing deformation in the simple shear is illustrated in Fig. 7. Again, the crystal c -axis distributions for non-recrystallizing, (a), and recrystallizing ice, (b), are shown. The results presented have

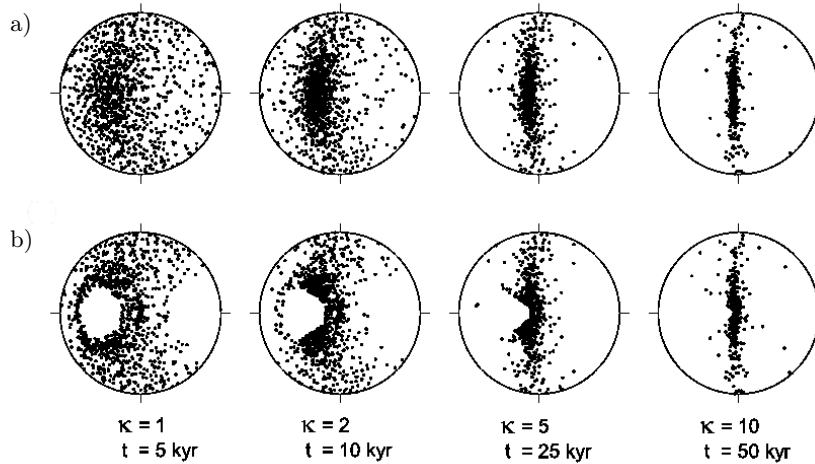


FIG. 7. Evolution of fabric in simple shear in the Ox_1x_3 plane as a function of the macroscopic shear strain κ and time t (in thousands of years) for: a) non-recrystallizing and b) recrystallizing ice.

been obtained by applying the hypothesis (2) for the new grain orientations, by which new grains have their c -axes initially inclined at the angle of 45° to the principal axis of the maximum macroscopic compressive stress. The same value of the critical equivalent stress $\zeta^{\text{cr}} = S_{\text{eq}}/\bar{S}_{\text{eq}} = 2.2$ as for the axial compression case has been adopted. Comparison of the diagrams in the upper and lower rows shows that the most significant differences between the fabrics developing in non-recrystallizing and recrystallizing ice occur at small shear strains κ . While only the lattice rotation mechanism operates, diagrams (a), the crystal c -axes first rotate towards the plane Ox_2x_3 (normal to the plane of the plot) and, for very large shear strains ($\kappa \gg 10$), start to cluster around the x_3 -axis, the latter becoming the principal axis of compression at $\kappa \rightarrow \infty$. In the case of the migration recrystallization mechanism being active, diagrams (b), the unfavourably oriented grains (those with the c -axes near the plane Ox_1x_3 and at the angles of about 45° to the x_3 -axis) are replaced by new grains, much better oriented for basal glide. These new grains, once getting around the x_3 axis, remain at this stable orientation, at which they do not undergo any further recrystallization. This contrasts with the uni-axial flow case, illustrated in Fig. 4b, in which the crystals repeatedly rotate toward the x_3 -axis, recrystallize, the newly created grains rotate again, recrystallize, and so on. The diagrams in Fig. 7b show that by the time the shear strain κ exceeds a magnitude of about 5, most of the crystals have already reached stable orientations near the plane Ox_2x_3 , so that further shearing does not cause any significant changes in the fabrics, which eventually become very close to those for non-recrystallizing ice at the same strain levels.

The fabrics predicted by the proposed model by applying the hypothesis (3) give qualitatively very similar patterns of c -axes distributions. On the other hand, the application of the hypothesis (1) predicts fabrics which differ from those in Fig. 7b. In that case, due to the restrictiveness of this hypothesis mentioned above, a large number of newly nucleated grain c -axes align at the same direction, coinciding with the direction of the maximum shear in the aggregate. Hence, the predicted fabrics feature very strong, point-like maxima (VAN DER VEEN and WHILLANS [22]), a property that seems to be unrealistic in the light of the field observations. (In the latter case, in order to better reproduce natural ice fabrics, one can introduce into the analysis some elements of randomness of the processes involved, but this is beyond the scope of this work.)

Figure 8 illustrates the variation of the dimensionless shear viscosities μ_{13}/μ_0 with increasing shear strain κ , obtained by employing the three hypotheses for the new grain initial orientation. Shown is also the variation of the shear viscosity for non-recrystallizing ice. We note a significant difference between the viscosity curves resulting from the application of the hypotheses (2) and (3) on one hand, and the hypothesis (1) on the other. The former two predict the be-

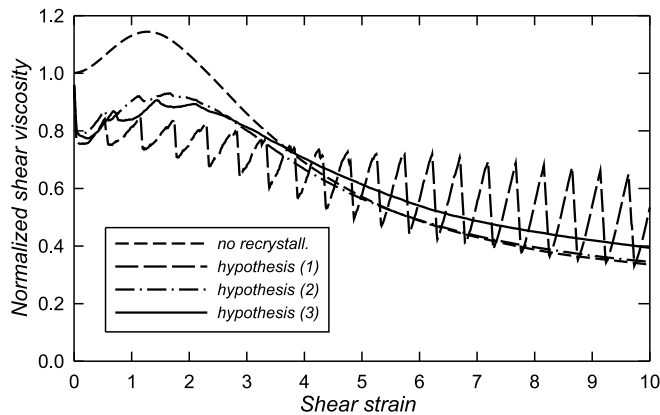


FIG. 8. Variation of the normalized shear viscosity μ_{13}/μ_0 with the shear strain κ in simple shearing for non-recrystallizing ice, and for recrystallizing ice with three different hypotheses on new crystal orientations.

behaviour in which, except the initial strain range $0 \leq \kappa \lesssim 2.5$, the viscosities vary in a smooth manner, with the curve for (2) approaching, for $\kappa \gtrsim 5$, that for non-recrystallizing ice. On the contrary, the hypothesis (1) predicts the behaviour in which the macroscopic shear viscosity curve has a saw-like shape, with regular, periodic changes in the viscosity magnitudes. The latter magnitudes vary significantly, as the maximum and minimum values within one ‘period’ differ by a factor of about two.

Finally, Fig. 9 demonstrates how the macroscopic shear viscosities μ_{13}/μ_0 are affected by the magnitude of the critical equivalent stress ζ^{cr} . Presented are

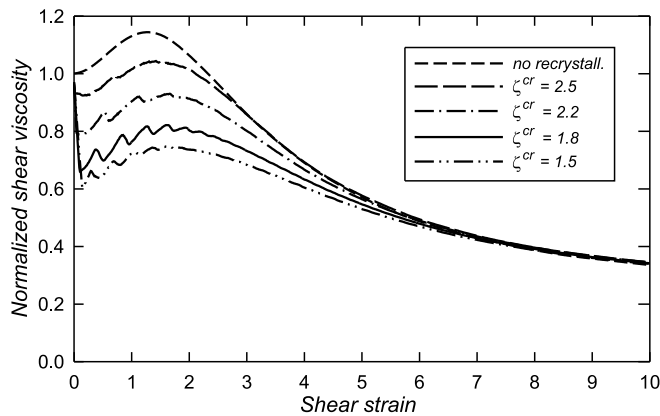


FIG. 9. Variation of the normalized shear viscosity μ_{13}/μ_0 with the shear strain κ in simple shearing for non-recrystallizing ice, and for recrystallizing ice with the hypothesis (2) on new crystal orientations, for different critical equivalent stresses ζ^{cr} .

the results obtained by adopting the hypothesis (2). It is seen that, irrespective of the critical stress level ζ^{cr} , the irregular changes in the viscosity values, reflecting the activity of recrystallization processes taking place on the microscopic level, are confined to the range of small shear strains, $\kappa \lesssim 2.5$. For larger strains, $\kappa \gtrsim 10$, the viscous response of the polycrystalline aggregate is practically insensitive to the magnitude of the stress controlling the onset of migration recrystallization. This indicates that the latter mechanism has a negligible effect on the fabric evolution once the majority of individual crystals have adjusted their orientations in such a way that they can deform mainly by basal glide.

5. Conclusions

The migration recrystallization mechanism in polar ice has been described by assuming that the process is controlled by the microscopic stress. Hence, recrystallize those crystals in which some critical level of the deviatoric stress invariant has been reached. The macroscopic response of ice has been derived by applying the Taylor-Voigt approximation of the velocity gradient uniformity in the polycrystalline aggregate.

The analysis of the microscopic stress dependence on the crystal c -axis orientation has shown that, due to the crystal anisotropy, the most favourable orientation of a grain within a polycrystal subjected to uni-axial compression differs, by a few degrees, from that commonly assumed in glaciology. The model predictions of the minimum and maximum micro-stresses in individual grains embedded in the polycrystalline aggregate agree very well with the results given by a more complex visco-plastic self-consistent formulation.

The proposed model reproduces well the qualitative features of anisotropic fabrics observed in natural ice masses; in particular, the girdle fabrics resulting from the recrystallization of ice under compression, and, to a smaller extent, the scattered fabrics forming in simple shear conditions. The numerical simulations predict the occurrence of recrystallization waves, reflected by periodic changes in the macroscopic viscosities in both the uni-axial compression and simple shear deformations. It has been found that the macroscopic axial viscosities of recrystallizing ice can be significantly smaller (by a factor of two) than those of the isotropic polycrystal. This indicates that the softening effect of migration recrystallization on the viscous behaviour of ice in compression is larger than that previously assumed. In simple shear, the softening effect of recrystallization occurs only at small strains.

Due to the difficulties associated with proper identification of physical quantities (such as the critical microscopic stress level or the recrystallization time of an individual grain), and also because of other simplifications introduced into the formulation, the proposed model certainly cannot aspire to offer a quan-

tatively accurate description of the migration recrystallization process in ice. Nonetheless, it is believed that, at the current stage of understanding of micro-mechanisms occurring in polar ice, the present formulation can provide results which are useful for large-scale ice sheet modelling applications, before more general, but tractable, theories, describing the thermodynamics of the recrystallization processes involved, have been developed.

References

1. R.B. ALLEY, *Flow-law hypotheses for ice-sheet modelling*, J. Glaciol., **38**, 129, 245–256, 1992.
2. N. AZUMA, A. HIGASHI, *Formation processes of ice fabric pattern in ice sheets*, Ann. Glaciol., **6**, 130–134, 1985.
3. W.F. BUDD, T.H. JACKA, *A review of ice rheology for ice sheet modelling*, Cold Reg. Sci. Technol., **16**, 2, 107–144, 1989.
4. O. CASTELNAU, P. DUVAL, R.A. LEBENSOHN, G.R. CANOVA, *Viscoplastic modeling of texture development in polycrystalline ice with a self-consistent approach: Comparison with bound estimates*, J. Geophys. Res., **101**, B6, 13,851–13,868, 1996.
5. S. DE LA CHAPELLE, O. CASTELNAU, V. LIPENKOV, P. DUVAL, *Dynamic recrystallization and texture development in ice as revealed by the study of deep ice cores in Antarctica and Greenland*, J. Geophys. Res., **103**, B3, 5091–5105, 1998.
6. P. DUVAL, *Creep and fabric of polycrystalline ice under shear and compression*, J. Glaciol., **27**, 95, 129–140, 1981.
7. P. DUVAL, L. ARNAUD, O. BRISSAUD, M. MONTAGNAT, S. DE LA CHAPELLE, *Deformation and recrystallization processes of ice from polar ice sheets*, Ann. Glaciol., **30**, 83–87, 2000.
8. P. DUVAL, O. CASTELNAU, *Dynamic recrystallization of ice in polar ice sheets*, J. Phys. IV, **5**, C3, 197–205, 1995.
9. S.H. FARIA, *Creep and recrystallization of large polycrystalline masses. III. Continuum theory of ice sheets*, Proc. R. Soc. Lond., A **462**, 2073, 2797–2816, 2006.
10. S.H. FARIA, G.M. KREMER, K. HUTTER, *On the inclusion of recrystallization processes in the modeling of induced anisotropy in ice sheets: a thermodynamicist's point of view*, Ann. Glaciol., **37**, 29–34, 2003.
11. S.H. FARIA, D. KJTITAREV, K. HUTTER, *Modelling evolution of anisotropy in fabric and texture of polar ice*, Ann. Glaciol., **35**, 545–551, 2002.
12. O. GAGLIARDINI, J. MEYSSONNIER, *Analytical derivations for the behavior and fabric evolution of a linear orthotropic ice polycrystal*, J. Geophys. Res., **104**, B8, 17,797–17,809, 1999.
13. G. GÖDERT, K. HUTTER, *Induced anisotropy in large ice shields: Theory and its homogenization*, Continuum Mech. Thermodyn., **10**, 5, 293–318, 1998.
14. A.J. GOW, D.A. MEESE, R.B. ALLEY, J.J. FITZPATRICK, S. ANANDAKRISHNAN, G.A. WOODS, B.C. ELDER, *Physical and structural properties of the Greenland Ice Sheet Project 2 ice core: A review*, J. Geophys. Res., **102**, C12, 26,559–26,575, 1997.

15. D. KTITAREV, G. GÖDERT, K. HUTTER, *Cellular automaton model for recrystallization, fabric, and texture development in polar ice*, J. Geophys. Res., **107**, B8, EPM 5, 2002.
16. J. MEYSSONNIER, A. PHILIP, *A model for tangent viscous behaviour of anisotropic polar ice*, Ann. Glaciol., **23**, 253–261, 1996.
17. L.W. MORLAND, *Influence of lattice distortion on fabric evolution in polar ice*, Continuum Mech. Thermodyn., **14**, 1, 9–24, 2002.
18. R. STAROSZCZYK, *A uniform strain, discrete-grain model for evolving anisotropy of polycrystalline ice*, Arch. Mech., **54**, 2, 103–126, 2002.
19. R. STAROSZCZYK, *Constitutive Modelling of Creep Induced Anisotropy of Ice*, IBW PAN Publishing House, Gdańsk, 2004.
20. R. STAROSZCZYK, L. W. MORLAND, *Strengthening and weakening of induced anisotropy in polar ice*, Proc. R. Soc. Lond., A **457**, 2014, 2419–2440, 2001.
21. T. THORSTEINSSON, J. KIPFSTUHL, H. MILLER, *Textures and fabrics in the GRIP ice core*, J. Geophys. Res., **102**, C12, 26,583–26,599, 1997.
22. C.J. VAN DER VEEN, I.M. WHILLANS, *Development of fabric in ice*, Cold Reg. Sci. Technol., **22**, 2, 171–195, 1994.

Received October 27, 2008; revised version February 21, 2009.
